Chemical Science

ROYAL SOCIETY OF CHEMISTRY

EDGE ARTICLE

View Article Online
View Journal | View Issue

Cite this: *Chem. Sci.*, 2026, **17**, 3171

All publication charges for this article have been paid for by the Royal Society of Chemistry

Received 10th November 2025
Accepted 12th December 2025

DOI: 10.1039/d5sc08731g

rsc.li/chemical-science

Diastereoselective synthesis of cyclopropyl sulfoxides *via* hydrosulfenation

Liyan Yuwen,† Jiazhong Tang,† Yayu Qi, Tianyi Zou, Shaotong Zhang, Ya-Qian Zhang and Qing-Wei Zhang *

Cyclopropyl sulfoxides, merging two privileged motifs in medicinal chemistry, remain synthetically challenging despite their pharmaceutical potential. Herein, we report a mild, metal-free hydrosulfenation strategy that enables their direct synthesis, achieving exceptional diastereoselectivity (dr up to > 20 : 1) in systems with up to eight possible diastereomers. Chiral sulfoxides with 4 to 7 stereogenic centers were also synthesized in high dr. The methodology provides direct access to medicinally relevant architectures, including cyclopropyl sulfones, sulfoximines, and drug-conjugated hybrids. Mechanistic studies reveal stereochemical control *via* collective spatial factors including *endo*/*exo*, facial and side selectivities during the cycloaddition step.

Introduction

Cyclopropane and sulfoxide moieties represent two privileged structural motifs in modern drug discovery, each endowing molecules with distinct physicochemical and pharmacological properties.[1–9] Systematic analyses of pharmaceutical compounds underscore their clinical significance: cyclopropane ranks as the 10th most prevalent ring system in marketed drugs,[10] while sulfur-containing structures appear in nearly 300 FDA-approved small-molecule therapeutics. Within this sulfur pharmacophore landscape, approximately 4% of these drugs incorporate the sulfoxide functional group.[11]

Given the significant individual contributions of cyclopropane and sulfoxide moieties to medicinal chemistry, exploring the potential of their combined structure, cyclopropyl sulfoxides, is highly compelling. This integration is anticipated to synergize the cyclopropane ring's rigid geometry and metabolic stability with the sulfoxide's ambident polarity and bioisosteric versatility, thereby rendering novel therapeutic profiles. Beyond their intrinsic value as potential bioactive entities, cyclopropyl sulfoxides serve as pivotal synthetic intermediates for accessing other sulfur-containing cyclopropane architectures. For instance, they can be oxidized to cyclopropyl sulfones or converted to cyclopropyl sulfoximines[12–17]—structural motifs present in clinically approved drugs[18] (Fig. 1a).

Despite this promising potential, the development of robust synthetic methods for cyclopropyl sulfoxides remains scarce. Among the limited potential approaches, sulfenic acid-mediated pathways represent a promising yet challenging route.[19–21] Sulfenic acids are highly transient species, prone to facile dimerization or disproportionation[22–25] (Fig. 1b). Their nucleophilic addition across unsaturated systems has been mainly documented with relatively electrophilic alkynes, while the corresponding reaction with alkenes remains virtually unexplored.[26–29] We thus envisioned extending this unconventional reaction mode to cyclopropenes.

However, the engagement of the electrically neutral, yet highly strained, cyclopropene π-system introduces distinct challenges.[30] The inherent ring strain, while a potential driver of reactivity, predisposes the system to ring-opening side reactions.[31–37] Furthermore, the simultaneous construction of multiple stereocenters in the product renders stereocontrol—particularly in non-metal-catalyzed systems—a formidable task (Fig. 1b). Conventional non-transition-metal-catalyzed mechanisms often involve stepwise ionic additions to the cyclopropene double bond, generating cyclopropyl cation or anion intermediates that subsequently react with nucleophiles or electrophiles.[38,39]

Herein, we report the hydrosulfenation of cyclopropenes to diastereoselectively synthesize cyclopropyl sulfoxides (Fig. 1c). In contrast to previous stepwise ionic pathways, the reaction proceeds through concerted cycloaddition between sulfenic acid intermediates and cyclopropenes. Moreover, excellent diastereoselectivity (dr up to > 20 : 1) over a potential pool of up to eight diastereomers was successfully achieved, governed by a well-defined hierarchy of spatial control elements during the cycloaddition transition state.

Results and discussion

To validate the proposed reaction pathway, we commenced our study by conducting the reaction with sulfoxide **1a** (as the

Key Laboratory of Precision and Intelligent Chemistry, Department of Chemistry, University of Science and Technology of China, Hefei 230026, China. E-mail: qingweiz@ustc.edu.cn

† These authors contributed equally to this work.

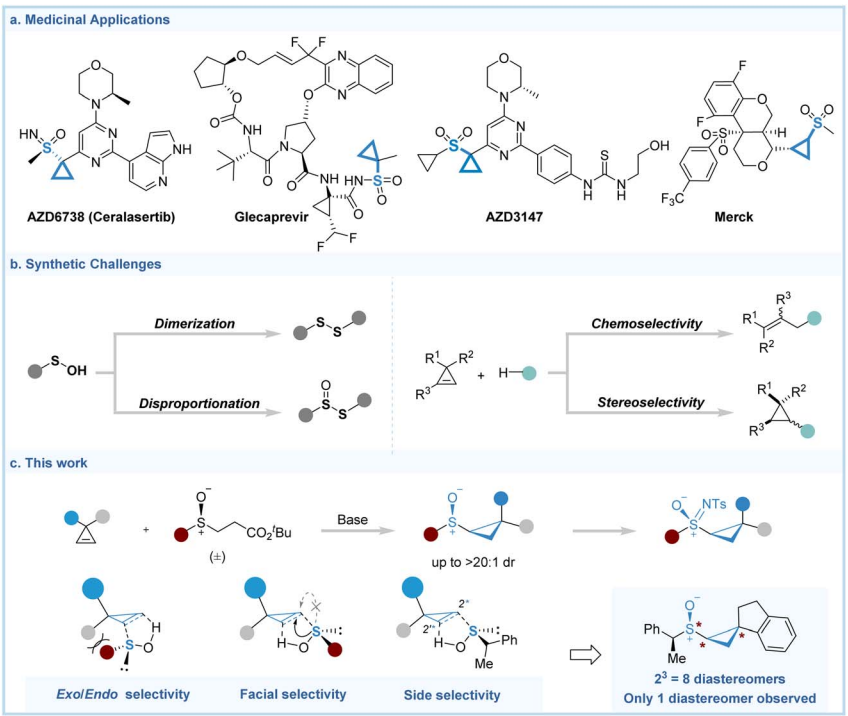

Fig. 1 Construction of cyclopropyl sulfoxides, applications and challenges.

sulfenic acid precursor) and cyclopropene **2m** as model substrates for initial optimization studies (see SI Table S1 online).

The extensive screening of reaction parameters revealed two critical determinants of reaction efficiency and selectivity. First, evaluation of bases demonstrated a significant influence on reaction efficiency, with weakly basic additives affording superior yields compared to strong bases. We hypothesize that gradual sulfenic acid release under mild basic conditions minimizes undesired side reactions, allowing efficient cyclopropene engagement. Second, steric differentiation between cyclopropene substituents emerged as the dominant factor governing diastereoselectivity. Introducing pronounced steric contrast dramatically enhanced stereocontrol. As a consequence, the optimal condition was identified as treating the sulfoxide and cyclopropene substrates with 1 equiv 4-methylmorpholine (NMM) in toluene (0.1 M) at 60 °C.

With the optimized reaction conditions established, we next explored the substrate scope of this reaction (Table 1). Initially, cyclopropene substrates bearing diverse substituents were investigated. A number of alkyl and aryl variants (**3a–3f**) delivered corresponding products in high yields (70–85%) with exceptional stereocontrol (dr > 20 : 1) over four pairs of possible diastereomers. In particular, the ferrocenyl group was proved compatible, with **3g** furnished in retained diastereoselectivity (dr > 20 : 1) albeit in moderated yield. Substrates with less hindered aromatic groups (*e.g.*, phenyl, naphthyl) afforded **3h–3n** in excellent yields (72–94%), though with attenuated stereoselectivity (dr 4 : 1 to 5 : 1).

To further demonstrate the versatility of this protocol, a broad scope of sulfenic acid precursors were examined. Sulfoxides bearing both weak electron-donating groups (**3p–3s**) and electron-withdrawing substituents (**3t–3x**) generated products efficiently (65–81% yield) without compromising diastereoselectivity (dr > 20 : 1), highlighting the reaction's tolerance to electronic perturbations. Alkyl sulfoxides also participated effectively, yielding **3y–3ab** with high efficiency (63–71% yield) and robust stereocontrol (dr 16 : 1 to >20 : 1). Collectively, these results establish a broad substrate compatibility as well as excellent diastereoselectivity spanning diverse cyclopropenes and sulfoxides. In particular, product **3ac** contains the same cyclopropyl amide structural fragment found in anti-depressant milnacipran.

Building upon the diastereoselective hydrosulfenation methodology, we next pursued the integration of sulfur-centered chirality[40–46] into this framework using enantioenriched sulfenic acid precursors and chiral cyclopropenes (Table 2). Combined with the strain-release desymmetrization strategy, a series of sulfur-stereogenic cyclopropyl sulfoxides (**4a–4m**) were synthesized with precise control over both the newly formed S-chirality and existing stereocenters. In particular, for substrates containing chiral benzylic groups, products (**4a–4i**) were obtained with complete retention of the original stereocenter configuration while simultaneously establishing three new stereogenic elements (S-center and two cyclopropane carbons), achieving exceptional diastereoselectivity (dr up to >20 : 1) among eight possible diastereomers.

Employing substrates with natural product fragments, including menthone derivatives (**4j**), dihydrocarvone derivatives (**4k**, **4k″**, two diastereomers shown), natural borneol derivatives (**4l**), and fructose derivatives (**4m**), compounds containing up to 7 stereocenters were successfully obtained in moderate yields.

Table 1 Substrate scope of cyclopropenes and racemic sulfoxides. Reaction conditions: 0.1 mmol sulfoxide, 0.11 mmol cyclopropene, 0.1 mmol NMM, 1 mL toluene and at 60 °C; 0.1 mmol scale with isolated yields; dr determined by molar ratio of isolated products

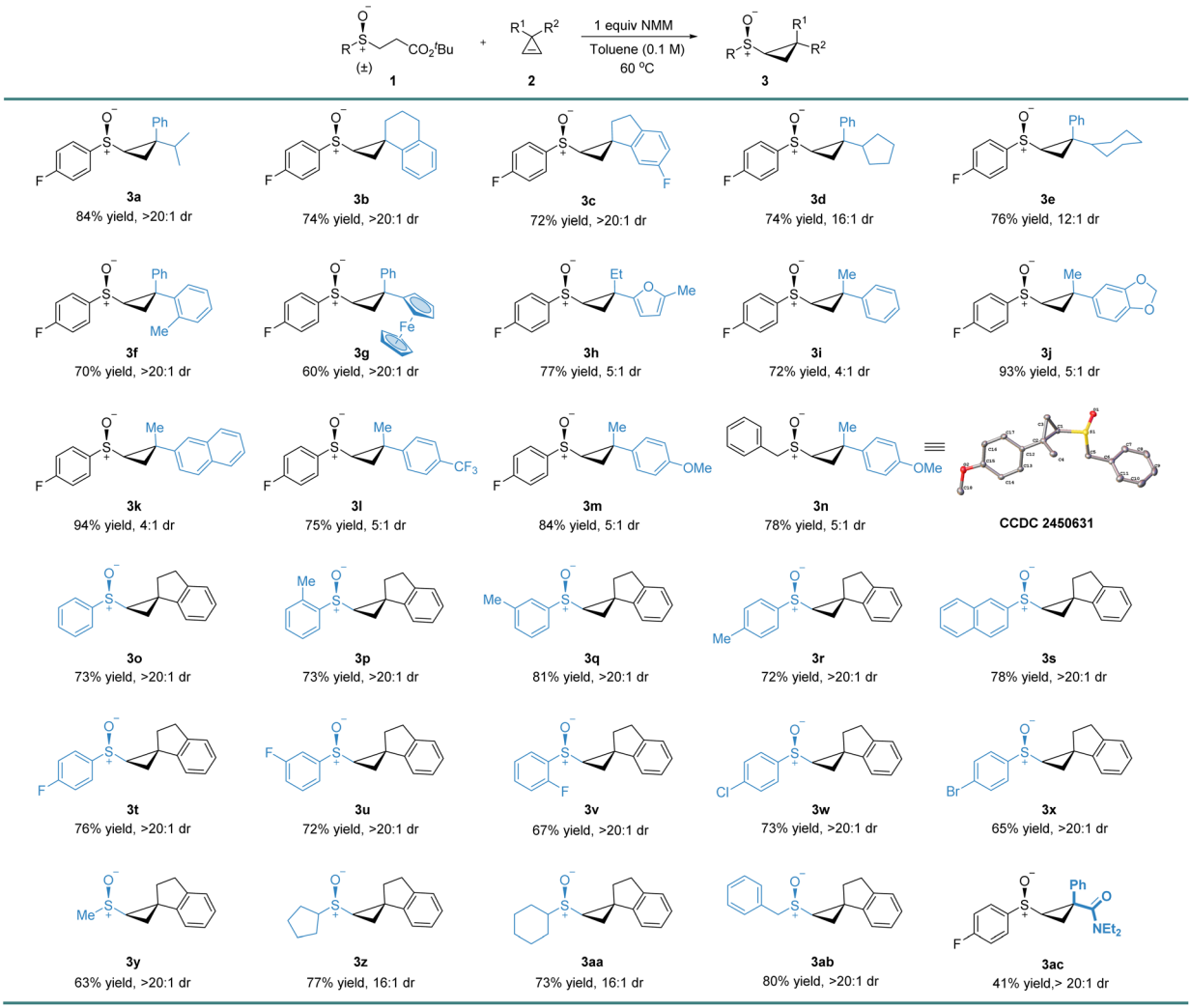

The preserved stereochemical integrity at sensitive positions underscores the mildness and selectivity of the strain-release activation mode.

The synthetic utility of this methodology was further exemplified through diversified post-functionalizations (Fig. 2). Gram-scale synthesis of **3t** (Fig. 2a) retained high efficiency (72% yield *vs.* 76% in small-scale) and stereoselectivity (dr > 20 : 1), confirming its excellent scalability for preparative applications. Subsequent methyl substitution at the sulfinyl-adjacent position was performed smoothly with moderate yields (Fig. 2b). Furthermore, sulfur-centric diversification was achieved by converting the sulfoxides into sulfoximines or sulfones, expanding accessible sulfur oxidation states and species. Oxidation to sulfone **5c** (Fig. 2c) proceeded in 56% yield with preserved diastereoselectivity (dr > 20 : 1).[47] For sulfoximines (Fig. 2d), the S=N bond was constructed *via* copper-catalysed nitrene transfer,[48,49] affording both **5d** and S-stereogenic **5e** in moderate yields (56% and 46%, respectively) with outstanding dr (>20 : 1). Finally, Pd-catalysed Suzuki cross-coupling with several drug molecules[50] furnished drug-conjugated hybrids **5f–5i** in high yields (70–99%) (Fig. 2e), demonstrating an easily accessible integration with complex pharmacophores. We believe these transformations have opened up a versatile platform for constructing stereochemically defined, functionally tunable cyclopropane architectures, with direct relevance to medicinal chemistry.

To elucidate the mechanistic underpinnings of stereochemical control in this transformation, we conducted density functional theory (DFT) calculations on the model reaction yielding product **4a**—a structure bearing four stereogenic elements (Fig. 3, **1***–**4***). The configurationally fixed **1*** center is inherited from the sulfoxide substrate **1o**, while **2***–**3*** emerge through cyclopropene desymmetrization during cycloaddition with sulfenic acid intermediate **Int-1**. The sulfur stereocenter (**4***) is dictated by the spatial geometry of this key bond-forming event. Collectively, these stereochemical determinants generate eight possible diastereomeric transition states (TS), corresponding to permutations of three variable stereochemical parameters beyond the fixed **1*** center (for details of all eight transition states **TS-2**–**TS-5**, please see SI).

Table 2 Substrate scope of chiral sulfoxides. Reaction conditions: 0.1 mmol sulfoxide, 0.11 mmol cyclopropene, 0.1 mmol NMM, 1 mL toluene and at 60 °C; 0.1 mmol scale with isolated yields; dr determined by molar ratio of isolated products

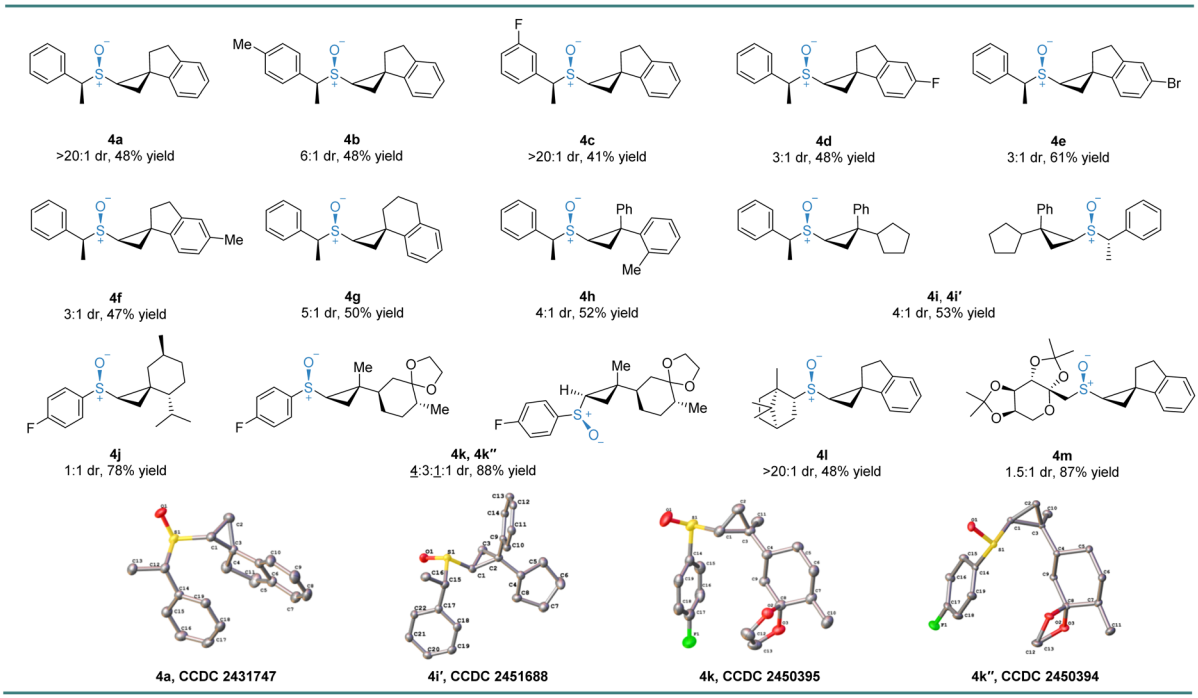

The reaction initiates with sulfoxide **1o** generating sulfenic acid intermediate **Int-1** through retro-Michael fragmentation, with an energy barrier of 26.1 kcal mol^{-1}. Subsequently, **Int-1** undergoes highly diastereoselective cycloaddition with benzannulated cyclopropene **2n** engaging three distinct stereochemical modulation pathways. The dominant stereodifferentiation arises from the sulfur substituent's spatial orientation during cycloaddition. While the reaction proceeds through a coplanar five-membered transition state involving the S–O–H moiety and alkene π-system, the benzyl substituent adopts either *endo* (the benzyl substituent inward) or *exo* (the lone pair inward) configurations. Severe steric repulsion in

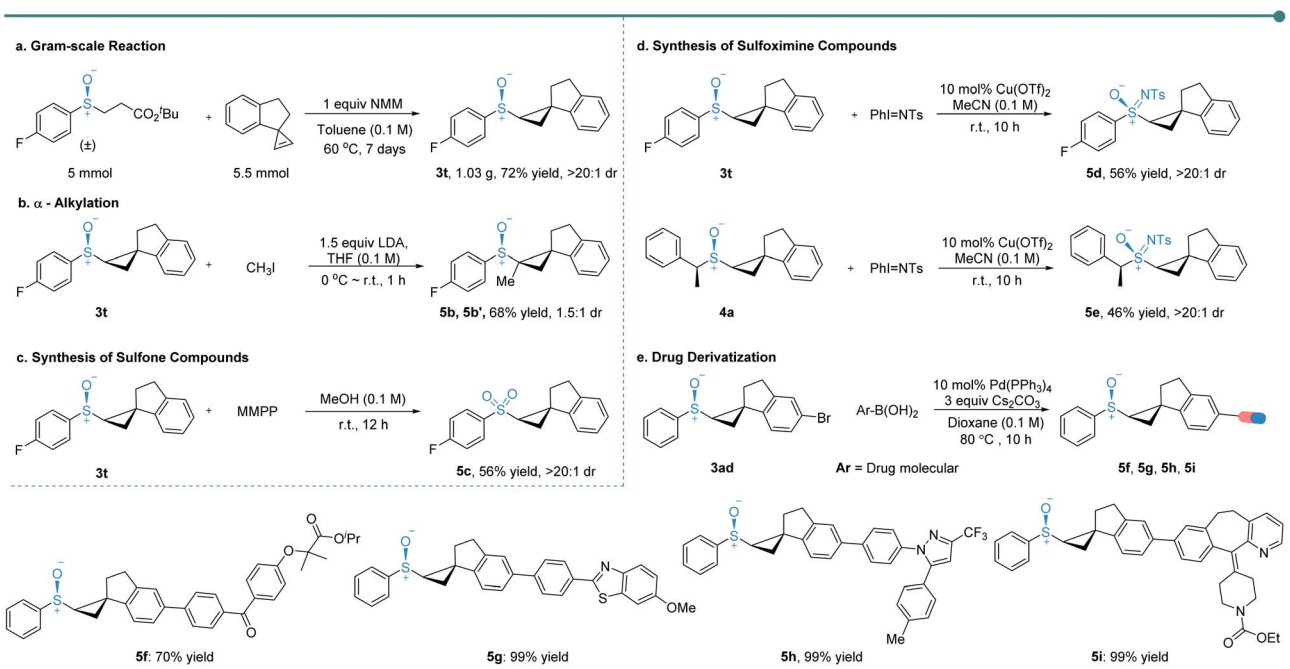

Fig. 2 Derivatization of the cyclopropyl sulfoxide product.

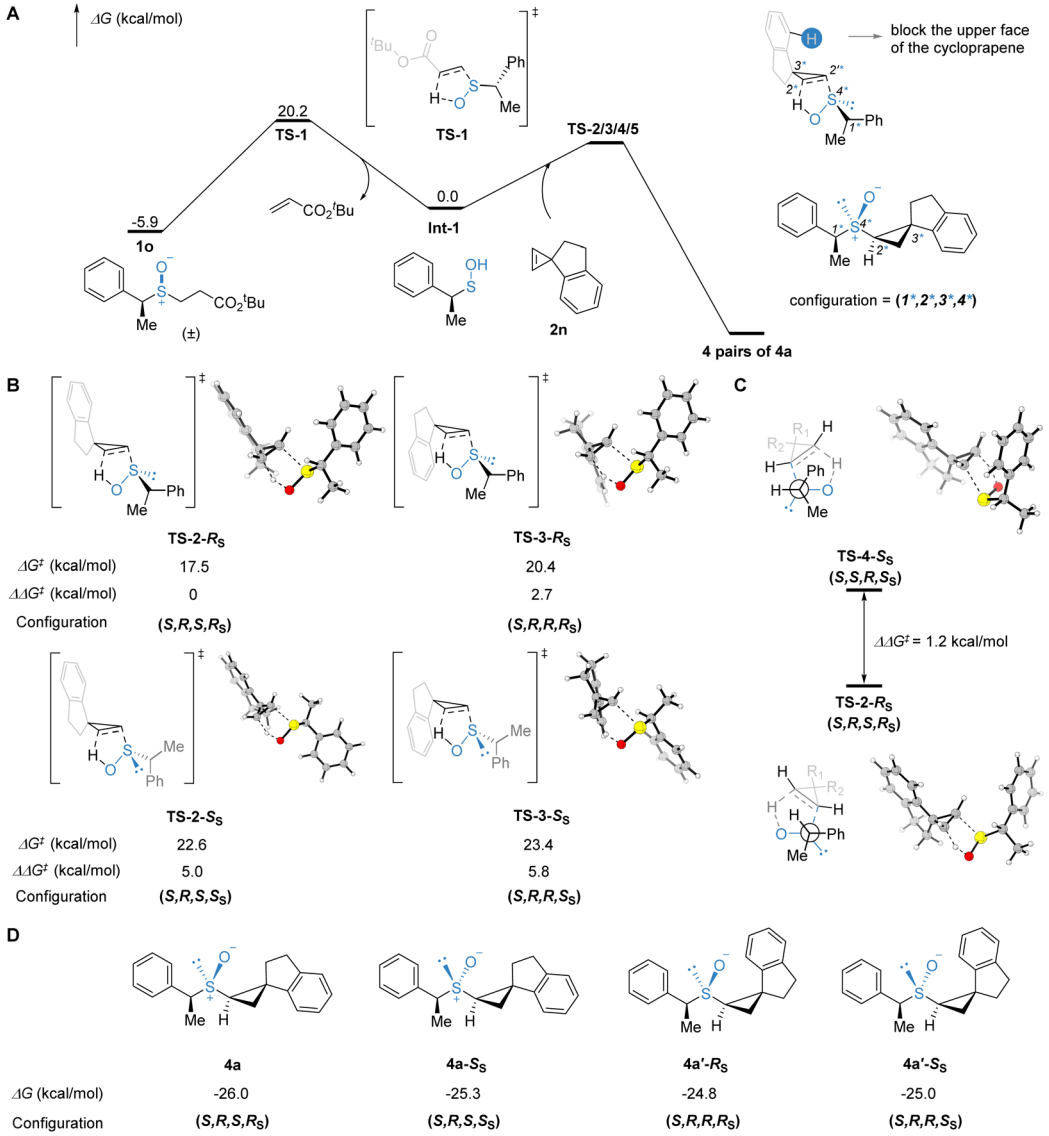

Fig. 3 Computational studies. DFT calculated reaction pathways at M062X/def2-TZVP/SMD(Toluene)//B3LYP-D3/def2-SVP level. All energies are in kcal mol^{-1}. (A): Overall energy profile. (B): Transition states regarding *endo*/*exo* and facial selectivity. (C): Side selectivity of carbon 2* *vs.* 2′*.

endo-type TSs elevates their energy by 5.0 kcal mol^{-1} relative to *exo*-counterparts (**TS-2-*Rs*** *vs.* **TS-2-*Ss***), establishing this as the primary stereochemical gatekeeper.

Beyond sulfur orientation, facial selectivity imposed by cyclopropene's rigid spiroindanyl group introduces secondary energy differentiation. Attack at the methylene face minimizes steric repulsion, whereas approach from the benzene face induces destabilizing repulsion originated from the C–H bond perpendicular to the π-system. A 2.7 kcal mol^{-1} energy gap was found between **TS-2-*Rs*** and **TS-3-*Rs***, rationalizing the observed facial preference.

Intriguingly, open-chain analog **4i** exhibit reversed facial selectivity, as confirmed by single-crystal X-ray analysis of **4i**'s two major diastereomers. This phenomenon may arise from the free rotation of the benzene ring that relieves allylic strain, thereby making the benzene face sterically less hindered than the cyclopentyl side. Consequently, the reaction preferentially occurs at the lower-energy benzene face. These results collectively demonstrate that facial selectivity is governed by substituent-induced steric profiles, with reactions favoring the sterically less encumbered face.

The residual stereochemical modulation stems from the side selectivity of enantiotopic cyclopropene carbons. While pseudo-enantiomeric pathways involving opposite cyclopropene carbons exhibit closely spaced energy profiles ($\Delta\Delta G^{\ddagger}$ = 1.2 kcal mol^{-1}, **TS-2-*Rs*** *vs.* **TS-4-*Rs***), the fixed **1*** center breaks this symmetry through differential van der Waals interactions at the cyclopropane–sulfoxide interface, thus determined the side selectivity (2* *vs.* 2′*).

Single-crystal X-ray diffraction unambiguously confirmed the structure of major diastereomer **4a**, which aligns with the lowest–energy transition state (methylene-face *exo* attack) predicted by DFT calculations. While computational models identified **4a″-*Ss***—the pseudo-enantiomer differing solely in

enantiotopic carbon selectivity—as the most probable minor product, its experimental isolation proved infeasible due to the exceptionally high diastereomeric ratio (dr > 20 : 1). To circumvent this limitation, we analyzed the stereochemical outcome of substrate **4i**. X-ray characterization of **4i**'s two predominant diastereomers revealed the pseudo-enantiomeric relationship expected for **4a** (between **4a** and **4a″-*Ss***), except for the benzene-face preference inherent to **4i**'s open-chain design (as rationalized in the facial selectivity analysis). This structural congruence validates our computational results, as both systems share identical stereochemical determinants despite divergent substitution patterns. The conserved configuration relationships across substrates demonstrate the generalizability of the stereocontrol model, particularly the dominance of sulfur orientation and facial selectivity.

Conclusions

In summary, we have developed a hydrosulfenation strategy for the synthesis of cyclopropyl sulfoxides using cyclopropenes, achieving excellent diastereoselectivity (dr up to > 20 : 1), high yields, and broad substrate scope under mild, metal-free conditions. The methodology provides direct access to structurally diverse cyclopropyl sulfoxides, which exhibit versatile post-functionalization potential, including oxidation to sulfones, conversion to sulfoximines, and integration with pharmacophores. Mechanistic studies revealed that the stereochemical outcome arises from a series of spatial control elements: dominant sulfur substituent orientation (*exo vs. endo*), followed by facial selectivity dictated by benzannulation-induced steric effects, and subtle side discrimination of enantiotopic carbons in substrates with fixed stereocenters. These factors collectively drive the preferential formation of low-energy transition states, with *exo* addition at the sterically less hindered face being energetically favored.

Data availability

All other data are available from the corresponding authors upon request.

CCDC 2450631, 2431747, 2451688, 2450394 and 2450395 contain the supplementary crystallographic data for this paper.[51a–e]

Supplementary information: optimization studies, experimental procedures, mechanistic studies, computational studies, NMR spectra and high-resolution mass spectrometry. See DOI: https://doi.org/10.1039/d5sc08731g.

Author contributions

Q.-W. Z. conceived the project and designed the experiments. L. Y. YW., Y. Y. Q. and S. T. Z. performed the experimental work. J. Z. T. conducted computational studies. T. Y. Z and L. Y. YW. wrote the manuscript.

Conflicts of interest

There is no conflict of interest to report.

Acknowledgements

This work was supported by NSFC (22471251, 22501268). The simulations and computational work were supported by the robotic AI-Scientist platform of Chinese Academy of Science and have been done on the Supercomputing Center of the University of Science and Technology of China. This work was partially carried out at the Instruments Center for Physical Science, University of Science and Technology of China.

Notes and references

1 A. De Meijere, *Angew. Chem., Int. Ed.*, 1979, **18**, 809–826.
2 S. S. Uthumange, A. J. H. Liew, X. W. Chee and K. Y. Yeong, *Bioorg. Med. Chem.*, 2024, **116**, 117980.
3 A. Gagnon, M. Duplessis and L. Fader, *Org. Prep. Proced. Int.*, 2010, **42**, 1–69.
4 C. M. Marson, *Chem. Soc. Rev.*, 2011, **40**, 5514–5533.
5 I. A. Novakov, A. S. Babushkin, A. S. Yablokov, M. B. Nawrozkij, O. V. Vostrikova, D. S. Shejkin, A. S. Mkrtchyan and K. V. Balakin, *Russ. Chem. Bull.*, 2018, **67**, 395–418.
6 D. Y.-K. Chen, R. H. Pouwer and J.-A. Richard, *Chem. Soc. Rev.*, 2012, **41**, 4631–4642.
7 U. Lücking, *Org. Chem. Front.*, 2019, **6**, 1319–1324.
8 C. Zhao, K. P. Rakesh, L. Ravidar, W.-Y. Fang and H.-L. Qin, *Eur. J. Med. Chem.*, 2019, **162**, 679–734.
9 E. Wojaczyńska and J. Wojaczyński, *Curr. Opin. Chem. Biol.*, 2023, **76**, 102340–102348.
10 R. D. Taylor, M. MacCoss and A. D. G. Lawson, *J. Med. Chem.*, 2014, **57**, 5845–5859.
11 K. A. Scott and J. T. Njardarson, *Top. Curr. Chem.*, 2018, **376**, 5.
12 M. Frings, C. Bolm, A. Blum and C. Gnamm, *Eur. J. Med. Chem.*, 2017, **126**, 225–245.
13 T. Bach and C. Körber, *Eur. J. Org Chem.*, 1999, **1999**, 1033–1039.
14 M. Zenzola, R. Doran, L. Degennaro, R. Luisi and J. A. Bull, *Angew. Chem., Int. Ed.*, 2016, **55**, 7203–7207.
15 H. Okamura and C. Bolm, *Org. Lett.*, 2004, **6**, 1305–1307.
16 T. Q. Davies, M. J. Tilby, J. Ren, N. A. Parker, D. Skolc, A. Hall, F. Duarte and M. C. Willis, *J. Am. Chem. Soc.*, 2020, **142**, 15445–15453.
17 X. Shen, Q. Liu, W. Zhang and J. Hu, *Eur. J. Org Chem.*, 2016, **2016**, 906–909.
18 Z. Časar, *Synthesis*, 2020, **52**, 1315–1345.
19 T. Z. Jia, M. N. Zhang, S. P. McCollom, A. Bellomo, S. Montel, J. Y. Mao, S. D. Dreher, C. J. Welch, E. L. Regalado, R. T. Williamson, B. C. Manor, N. C. Tomson and P. J. Walsh, *J. Am. Chem. Soc.*, 2017, **139**, 8337–8345.
20 F. Saito, *Synthesis*, 2024, **56**, 220–228.
21 L. Gao, Y. Q. Wang, Y.-Q. Zhang, Y. H. Fu, Y. Y. Liu and Q.-W. Zhang, *Angew. Chem., Int. Ed.*, 2024, **63**, e202317626.

22 C. M. A. Gangemi, E. D'Agostino, M. C. Aversa, A. Barattucci and P. M. Bonaccorsi, *Tetrahedron*, 2023, **143**, 133550.
23 S. E. Leonard, K. G. Reddie and K. S. Carroll, *ACS Chem. Biol.*, 2009, **4**, 783–799.
24 V. Gupta, J. Yang, D. C. Liebler and K. S. Carroll, *J. Am. Chem. Soc.*, 2017, **139**, 5588–5595.
25 S. L. Scinto, O. Ekanayake, U. Seneviratne, J. E. Pigga, S. J. Boyd, M. T. Taylor, J. Liu, C. W. Am Ende, S. Rozovsky and J. M. Fox, *J. Am. Chem. Soc.*, 2019, **141**, 10932–10937.
26 D. N. Neville Jones, P. D. Cottam and J. Davies, *Tetrahedron Lett.*, 1979, **20**, 4977–4980.
27 A. V. Kalyanakrishnan, A. Joshy, A. K. Arya and A. Kaliyamoorthy, *ChemistrySelect*, 2021, **6**, 14054–14059.
28 Y.-Q. Zhang, L. F. Hu, L. Y. Yuwen, G. Lu and Q.-W. Zhang, *Nat. Catal.*, 2023, **6**, 487–494.
29 L. J. Alcock, K. D. Farrell, M. T. Akol, G. H. Jones, M. M. Tierney, H. B. Kramer, T. L. Pukala, G. J. L. Bernardes, M. V. Perkins and J. M. Chalker, *Tetrahedron*, 2018, **74**, 1220–1228.
30 R. Vicente, *Chem. Rev.*, 2021, **121**, 162–226.
31 A. K. Griffith, C. M. Vanos and T. H. Lambert, *J. Am. Chem. Soc.*, 2012, **134**, 18581–18584.
32 S. Ni, J. Chen and S. Ma, *Org. Lett.*, 2013, **15**, 3290–3293.
33 H. Fang, L. Yuwen, Y. Qi, J. Wang and Q.-W. Zhang, *Synlett*, 2025, **36**, 1780–1784.
34 S. Nie, A. Lu, E. L. Kuker and V. M. Dong, *J. Am. Chem. Soc.*, 2021, **143**, 6176–6184.
35 S. Wang, X. Li, J. Song and X. Fang, *Org. Chem. Front.*, 2025, **12**, 3223–3229.
36 A. Ali, C. Chung, J. Wang, L. Liu, Y. Kong, C. Wang, Y. Liu, Q. Yin and S. Lin, *Org. Lett.*, 2025, **27**, 740–746.
37 J. Han, Y. Liu, X. Yang, X. Zhang, Y. Zhu, M. Zhao, G. Hao and Y. Jiang, *Org. Chem. Front.*, 2023, **10**, 4887–4894.
38 J. García-Lacuna, G. Domínguez, Á. M. Martínez and J. Pérez-Castells, *Org. Chem. Front.*, 2025, **12**, 2525–2551.
39 P. Li, X. Zhang and M. Shi, *Chem. Commun.*, 2020, **56**, 5457–5471.
40 L. Wang, M. Chen, P. Zhang, W. Li and J. Zhang, *J. Am. Chem. Soc.*, 2018, **140**, 3467–3473.
41 M. J. Tilby, D. F. Dewez, A. Hall, C. Martínez Lamenca and M. C. Willis, *Angew. Chem., Int. Ed.*, 2021, **60**, 25680–25687.
42 X. Zhang, E. C. X. Ang, Z. Yang, C. W. Kee and C.-H. Tan, *Nature*, 2022, **604**, 298–303.
43 S. Huang, Z. Zeng, N. Zhang, W. Qin, Y. Lan and H. Yan, *Nat. Chem.*, 2023, **15**, 185–193.
44 M. Liao, Y. Liu, H. Long, Q. Xiong, X. Lv, Z. Luo, X. Wu and Y. R. Chi, *Chem*, 2024, **10**, 1541–1552.
45 Z. Peng, S. Sun, M.-M. Zheng, Y. Li, X. Li, S. Li, X.-S. Xue, J. Dong and B. Gao, *Nat. Chem.*, 2024, **16**, 353–362.
46 T. Wei, H.-L. Wang, Y. Tian, M.-S. Xie and H.-M. Guo, *Nat. Chem.*, 2024, **16**, 1301–1311.
47 M. H. Ali and G. J. Bohnert, *Synth. Commun.*, 1998, **28**, 2983–2998.
48 P. Brandt, M. J. Södergren, P. G. Andersson and P.-O. Norrby, *J. Am. Chem. Soc.*, 2000, **122**, 8013–8020.
49 D. Leca, K. Song, M. Amatore, L. Fensterbank, E. Lacôte and M. Malacria, *Chem.–Eur. J.*, 2004, **10**, 906–916.
50 D. L. Orsi, B. J. Easley, A. M. Lick and R. A. Altman, *Org. Lett.*, 2017, **19**, 1570–1573.
51 (*a*) CCDC 2450631: Experimental Crystal Structure Determination, 2025, DOI: 10.5517/ccdc.csd.cc2n82mn; (*b*) CCDC 2431747: Experimental Crystal Structure Determination, 2025, DOI: 10.5517/ccdc.csd.cc2mmfg5; (*c*) CCDC 2451688: Experimental Crystal Structure Determination, 2025, DOI: 10.5517/ccdc.csd.cc2n95qw; (*d*) CCDC 2450394: Experimental Crystal Structure Determination, 2025, DOI: 10.5517/ccdc.csd.cc2n7tzq; (*e*) CCDC 2450395: Experimental Crystal Structure Determination, 2025, DOI: 10.5517/ccdc.csd.cc2n7v0s.